

Soft Matter

Accepted Manuscript



This is an *Accepted Manuscript*, which has been through the Royal Society of Chemistry peer review process and has been accepted for publication.

Accepted Manuscripts are published online shortly after acceptance, before technical editing, formatting and proof reading. Using this free service, authors can make their results available to the community, in citable form, before we publish the edited article. We will replace this *Accepted Manuscript* with the edited and formatted *Advance Article* as soon as it is available.

You can find more information about *Accepted Manuscripts* in the [Information for Authors](#).

Please note that technical editing may introduce minor changes to the text and/or graphics, which may alter content. The journal's standard [Terms & Conditions](#) and the [Ethical guidelines](#) still apply. In no event shall the Royal Society of Chemistry be held responsible for any errors or omissions in this *Accepted Manuscript* or any consequences arising from the use of any information it contains.

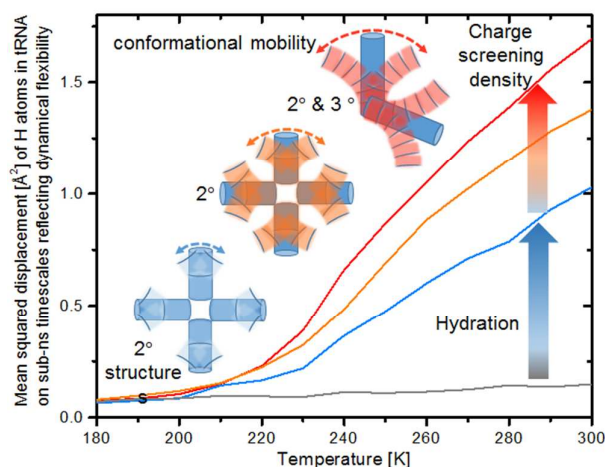
Graphical abstract for Soft Matter

Charge screening in RNA: An integral route for dynamical enhancements

Joon Ho Roh,^{*a,b} Madhu Tyagi,^{c,d} Pulakesh Aich,^a Kimoon Kim,^{a,e,f} R. M. Briber,^d Sarah A. Woodson^g

^aCenter for Self-assembly and Complexity, Institute for Basic Science, Pohang, South Korea; ^bBiomolecular Science, University of Science and Technology, Daejeon, South Korea; ^cNIST Center for Neutron Research, National Institute of Standards and Technology, Gaithersburg, Maryland 20899, USA; ^dDepartment of Materials Science and Engineering, University of Maryland, College Park, Maryland 20742, USA; ^eDepartment of Chemistry, Pohang University of Science and Technology, Pohang, South Korea; ^fDivision of Advanced Materials Science, Pohang University of Science and Technology, Pohang, South Korea; ^gJenkins Biophysics Department, Johns Hopkins University, Baltimore, Maryland 21218, USA

*Corresponding author
Email: jhroh@ibs.re.kr



Greater charge-screening density facilitates additional conformational mobility of hydrated tRNAs on sub-nanosecond timescales, while it renders global structures more stable.



Soft Matter

COMMUNICATION

Charge screening in RNA: An integral route for dynamical enhancements

Received 00th January 20xx,
Accepted 00th January 20xx

Joon Ho Roh,^{a,b} Madhu Tyagi,^{c,d} Pulakesh Aich,^a Kimoon Kim,^{a,e,f} R. M. Briber^d and Sarah A. Woodson^g

DOI: 10.1039/x0xx00000x

www.rsc.org/

Electrostatic interactions of RNA are in the center of determining the dynamical flexibility and structural stability. By analysing neutron scattering spectroscopy, we show that fast dynamics of hydrated tRNA on ps to ns timescales increases with stronger charge screening, while its structural stability either increases or remains largely unchanged. An unprecedented electrostatic threshold for the onset of additional flexibility is induced from the correlation between the charge-screening density of counterions and the promoted dynamical properties. The results demonstrate that the enhanced dynamical flexibility of tRNA originates from local conformational relaxation coupled with stabilized charge screening rather than governed by fluctuation of hydrated counterions. The present study casts light on the specificity of electrostatic interactions to thermodynamic balance between dynamical flexibility and structural stability of RNA.

Biological macromolecules have evolved to serve their functions in accord with gene-commanded responses to endo- and exo-cellular environments. Dynamical interactions of biological macromolecules (in particular, RNAs and proteins) with solvents and hydrated solutes are an integral part of their functional adaptation in a variety of biological events, including enzymatic reaction¹ and folding nucleation². However, understanding the conformational dynamics of biological macromolecules is non-trivial since surrounding environments lead to a complex contribution to it through electrostatic, hydration, or/and structure stabilizing interactions (hydrophobic for proteins and sequence-specific tertiary for RNA).

According to previous neutron scattering and simulation

studies, conformational dynamics of proteins is strongly coupled with diffusive motions of hydrating water molecules.³ More recently, our neutron scattering and dielectric studies on the dynamics of hydrated proteins and RNAs showed that the coupled motions are attributed to mutual response between chemical structures of biopolymers and their interactions with water rather than controlled by dynamics of hydrating water.^{4(b),5}

However, as compared with neutral and weakly charged proteins, understanding the dynamics of RNA remains more challenging in that electrostatic neutralization of the negatively charged nucleic acids stabilizes the compact folded structure of RNA, while helping to increase the molecular mobility of the biological polyelectrolytes.^{1(c),1(d)} Therefore, the dynamics of RNA must be described in the context of the specificity of charge screening to thermodynamic link between dynamical electrostatic interactions and structural stabilization.⁶ More satisfactory understanding of the charge-screening mediated connection between dynamical flexibility and structural stability requires detailed examination of the effects of the strength of charge screening on the dynamical enhancements of hierarchically structured RNA samples.

This communication presents that pico- to nano-second conformational mobility of hydrated tRNA that translates into a dynamic energy factor is enhanced by larger charge-screening density of hydrated counterions, while it stabilizes RNA secondary or tertiary structures. This result suggests that the additional conformational mobility of tRNA is coupled with stabilized charge screening rather than the fluctuation of hydrated counterions. We also found a new turnover for the onset of additional conformational dynamics, which is ascribed to an electrostatic threshold evaluated from the correlation between charge-screening density of counterions and the increased dynamic energy factors.

Wheat germ tRNA samples were used for this study. Details about sample preparation including the deuteration of labile protons in tRNA, the addition of salts (MgCl₂, NaCl, KCl), and hydration are described in the ESI. The mole ratio (m) of each salt to phosphate groups of the tRNA was 30. The

^aCenter for Self-assembly and Complexity, Institute for Basic Science, Pohang, South Korea; ^bBiomolecular Science, University of Science and Technology, Daejeon, South Korea; ^cNIST Center for Neutron Research, National Institute of Standards and Technology, Gaithersburg, Maryland 20899, USA; ^dDepartment of Materials Science and Engineering, University of Maryland, College Park, Maryland 20742, USA; ^eDepartment of Chemistry, Pohang University of Science and Technology, Pohang, South Korea; ^fDivision of Advanced Materials Science, Pohang University of Science and Technology, Pohang, South Korea; ^gJenkins Biophysics Department, Johns Hopkins University, Baltimore, Maryland 21218, USA.

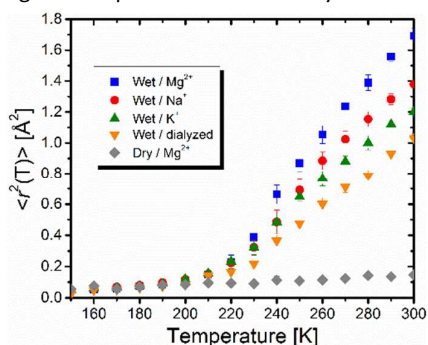
*Corresponding author; Email: jhroh@ibs.re.kr

Electronic Supplementary Information (ESI) available: [details of any supplementary information available should be included here]. See DOI: 10.1039/x0xx00000x

equimolar was chosen among the salts to explore concomitant variation of dynamics with 1) the strength of charge screening, 2) the charge density of hydrated counterions, 3) equivalent hydration, and 4) hierarchical structural stabilization. The charge density of hydrated counterions reflects relative difference in total electrostatic screening, whereby referred to as charge-screening density. Structural studies employing small-angle X-ray scattering spectroscopy verified that the addition of 30m Mg^{2+} enables tRNA to fold into compact native structures with the formation of tertiary interactions, while it remains extended secondary conformations with only monovalent counterion Na^+ or K^+ .^{6,7} Hydration of tRNA samples was conducted under 100% D_2O humidity in a desiccator. The extent of hydration for wet samples was 0.65h (h : the weight of hydrating water in grams / 1 g tRNA) which corresponds to a single hydration layer. The difference in total amount of hydrating water caused by the presence of additional 30 m Cl⁻ for $MgCl_2$ is estimated to be $< 0.02h$. Dry sample contains small amount of water corresponding to $\sim 0.05h$ after 48 hours of lyophilization under 0.3 mTorr. Elastic scattering scans were carried out on HFBS (NG2 at the NIST Center for Neutron Research) at a rate of 0.7 K/min between 50 and 320 K. Dynamic scattering spectra were collected in the energy window of 17 μeV and the resolution of 0.8 μeV , which cover the time range from 40 ps to 2 ns.

Fig. 1 shows temperature variations of mean-squared displacements, $\langle r^2(T) \rangle$, of hydrogen atoms in dry and wet tRNA samples with or without counterions. It is estimated using the following equation, $\langle r^2(T) \rangle = -3Q^2 \ln[I_{el}(Q,T)/I_{el}(Q,4K)]$, where I_{el} is the elastic neutron scattering intensity. The $\langle r^2(T) \rangle$ provides information about the damped local motions faster than the resolution ~ 2 ns including segmental, secondary dynamics, and the collective vibrations.

The temperature dependence of $\langle r^2(T) \rangle$ reveals that all wet tRNA samples exhibit a dynamic transition for the onset of anharmonic motions, defined as the sudden rise of $\langle r^2(T) \rangle$, at $T \sim 210$ K, while it is absent in the dry sample. Given that the onset of the conformational relaxation is coupled with dynamics of hydrating water,³ the similarity of dynamic transition temperatures (T_d) suggests that the extent of hydration-induced dynamical enhancements little changes regardless of the addition of the salts. The T_d would otherwise shift to higher temperatures for less hydration as reported



previously.⁵

Fig. 1 Mean-squared displacements, $\langle r^2(T) \rangle$, of H-atoms in tRNA samples. Error bars represent standard deviations.

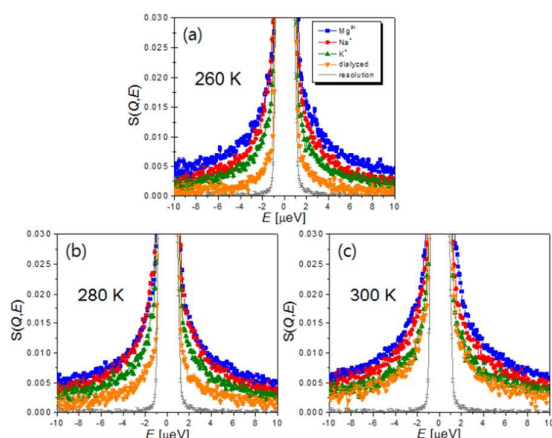
The thermal scanning of the UV-absorption at 260 nm shows that Mg^{2+} -tRNA sample folds into 3D structures (Fig. S1). In contrast, Na^+ - and K^+ -tRNA samples hold mostly secondary structures with lack of long-range tertiary interactions since the monovalent cations offer cationic charges as half as that of the Mg^{2+} (Fig. S1).⁶ The largest $\langle r^2(t) \rangle$ in Mg^{2+} -tRNA reflects the greatest flexibility, while it has the most compact folded structures.⁷ Interestingly, flexibility of the other tRNA samples becomes larger in the order of $Na^+ > K^+ >$ dialyzed (Fig. 1), while the structural stability is slightly increased in the presence of the monovalent cations, but remains largely unchanged between them. The above results show that stronger electrostatic interactions attributed to greater charge density of hydrated counterions (Table 1) are a key factor in enhancing dynamic collective motions of tRNA upon charge screening. Larger scale motions are probably coupled with the spatial ranges of stabilized charge screening rather than governed by entropic fluctuation of hydrated cations in which case relatively loosely bound K^+ would result in greater flexibility of tRNA like plasticizers: more flexibility of RNA with more strongly bound counterions upon hydration. It is worth noting that larger $\langle r^2(t) \rangle$ of Na^+ -tRNA than that of K^+ -tRNA despite their similar structures evidences that the dependence of fast dynamics on charge-screening density is stronger than that of structural interactions. This is consistent with our earlier results reporting similar flexibility between RNA and synthetic polyelectrolytes⁶.

Since sole analysis of $\langle r^2(T) \rangle$ is not able to discriminate among the different motions, we measure energy-resolved spectra covering 40 ps to 2 ns. Fig. 2 shows dynamic structure factors summed over all Q . As consistent with the results of $\langle r^2(T) \rangle$, the broadening of Quasi-Elastic Neutron Scattering (QENS) become larger following the same order as $Mg^{2+} > Na^+ > K^+ >$ dialyzed at all three temperatures. This again confirms that Mg^{2+} -induced charge screening results in greater conformational flexibility of the RNA accessed in the time window (Fig. 2). QENS spectra were fit to a function representing the deconvolution of the total scattering spectrum into an elastic and a quasielastic function which correspond respectively to the scattering of immobile H-atoms and relaxation motions of mobile fraction: $S(Q,E) = DW(Q)[EISF(Q)\delta(E) + QISF(Q)L(I,E)] \otimes R(E)$, where \otimes signifies convolution, and $L(I,E) = \pi^{-1} [I' / (E^2 + I'^2)]$. The DW , L , I' , and $R(E)$ are the Debye-Waller factor, a Q -dependent Lorentzian function, the half-width at half-maximum of the QENS peak, and a resolution function, respectively. The $EISF(Q)$ and $QISF(Q)$ denote the elastic and quasi-elastic incoherent scattering factor.

The relaxation rates are assessed with a single Lorentzian function (An example of the QENS analysis with a single Lorentzian function is exhibited in Fig. S2.). For the rationale behind the approximation of the relaxation spectrum as Lorentzian function, please see references 6 and 8. In Fig. 3A temperature variations of the relaxation times show slight non-Arrhenius behaviour indicating cooperative conformational motions. The average relaxation rate of tRNA

becomes faster with hydrated counterions of larger charge-

tRNA traced by QENS is believed to originate from the average



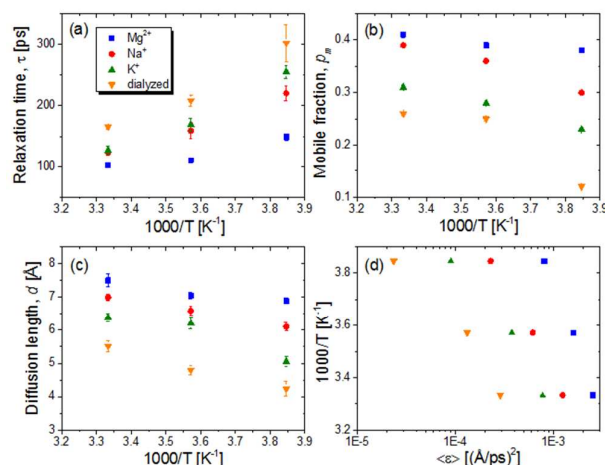
screening density at temperatures between 260 and 300 K.

Fig. 2 $S(Q,E)$ summed over all Q ranges of wet tRNA samples at $T =$ (a) 260 K, (b) 280 K, and (c) 300 K. Resolution function is Na^+ -tRNA at 10 K.

Partitioning of the hydrogen atoms into conformational relaxation, and their diffusive distance are characterized from Q -dependent fit of a model representing diffusion in a sphere to $EISF(Q) = 1 - p_m + p_m[3j_1(Qd)/(Qd)]^2$, where p_m and d are mobile fraction and the radius of sphere (Fig. S3). Dialyzed tRNA exhibits a second decay in the $EISF(Q)$ at higher $Q \sim 1.3 \text{ \AA}^{-1}$ ($\sim 4 \text{ \AA}$), which does not appear for all counterions mediated tRNA samples. Though beyond the scope of this paper, this implies that more localized motions also exist distinctively in the unscreened structures, probably originating from local structures loosely constrained by weaker electrostatic repulsion formed by sparse surrounding negative charges. The present study focuses on the analysis of larger scale motions emerging at lower Q , of which nature is comparable to the relaxation observed in salted tRNA samples, and presumably more likely to be affected by the electrostatic interactions.

The resulting values of p_m and d are plotted against inverse temperatures (Fig. 3B and 3C). The p_m of Mg^{2+} -tRNA turns out larger than Na^+ - and K^+ -tRNA, ranging from 0.38 at 260 K to 0.41 at 300 K. Since the accessed timescales are too limited to characterize full distribution of relaxation, the estimated p_m does not represent total fraction of mobile hydrogen atoms. Strong increase of temperature-dependent p_m is observed in Na^+ -tRNA, reaching 0.39 at 300 K which is very similar to the p_m of Mg^{2+} -tRNA. The relaxation length scale, d , of Mg^{2+} -tRNA is also greater than that of other counterions mediated tRNAs at the temperature ranges between 260 and 300 K. The d of the folded Mg^{2+} -tRNA is $\sim 7.5 \text{ \AA}$ at 300 K, which reflects the relaxation of its localized structures involving $\sim 40\%$ of total hydrogen atoms ($p_m \sim 0.4$). The spatial range of the localized motions are about 50% and 20% of the size of its helical unit and global structure.⁵

MD simulation and NMR studies revealed that hinge motions emerge from the bulges or helix junctions in HIV transactivation response (TAR) RNA on nanosecond timescales.⁹ Similar to the hinge motions, the fast dynamics of



localized motions related to inter-secondary structures between the acceptor stem and the T ψ C loop stem, or between the anticodon stem and the D loop stem.⁵

Fig. 3 Dynamic parameters obtained from the analysis of quasielastic dynamic structure factor: (a) τ ; (b) p_m ; (c) d . The τ values are calculated from Γ values of quasielastic Lorentzian relaxation functions and averaged over Q ranges between 0.87 \AA^{-1} and 1.68 \AA^{-1} where no Q -dependence of τ is observed. The (d) shows the variation of fractional dynamic energy factors with inverse temperatures.

As it shows lower $\langle r^2(T) \rangle$ at T above T_d , the K^+ -tRNA has the local conformational motions of smaller p_m and d than Na^+ -tRNA at all temperatures. For dialyzed tRNA, the most remarkable result is decrease of p_m down to ~ 0.1 at 260 K while it remains larger than 0.2 for salted samples. This indicates that the electrostatic repulsion drastically reduces thermally mobile segments as temperature is near $T_d \sim 210 \text{ K}$.

Energetic assessment of dynamical flexibility pertaining to complicated molecular motions of biopolymers is not trivial and requires understanding of several dynamical parameters.⁵ To follow the energetic variation associated with the fast conformational relaxation of tRNA, we introduce an averaged fractional dynamic energy factor, $\langle \epsilon \rangle$ expressed by combining the three dynamic parameters: d , τ , and p_m : Fractional $\langle \epsilon \rangle \sim \frac{\sum N v^2}{\sum N} \sim p_m \left(\frac{d}{\tau}\right)^2$. (Note: The term “relative” describes the weighing of p_m which accesses the part of total energy.) The presentation of the comprehensive dynamic property $\langle \epsilon \rangle$ is attempted to evaluate relative kinetic energy of the locally diffusive motions of H-atoms in tRNA samples.

Fig. 3D shows that the calculated $\langle \epsilon \rangle$ values nonlinearly vary with temperature (for an ideal case, thermal and dynamic energy are linearly dependent with a pre-factor 2/3), reflecting cooperative segmental relaxation. Shift of temperature variation of the $\langle \epsilon \rangle$ to larger values with greater charge-screening density indicates that the dynamical flexibility pertaining to conformational relaxation of tRNA is enhanced by stronger charge screening.

The greater flexibility induced by ionizing salts was reported for halophilic proteins such as malate dehydrogenase

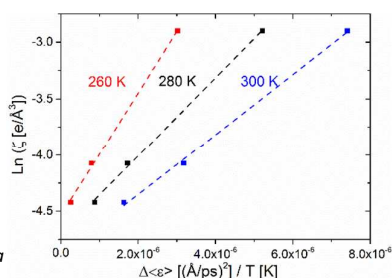
and 2Fe-2S ferredoxin from *Haloarcula marismortis*, which also consist of highly negative surface charge densities¹⁰. However, the structural stability of the proteins varies with different types of salts because of thermodynamic difference in their interactions with water and the subsequent solvated structures: Salting-in salts (Kosmotropic) stabilize the proteins, but salting-out (Chaotropic) destabilize at molar concentrations. Since the thermodynamic interplays become more complex for biologically important, intermediate salts including NaCl and KCl, the specificity of electrostatic interactions to the balance between dynamic flexibility and structural stability has not been straightforwardly evaluated for the halophilic proteins.¹⁰

Likewise, the role of charge screening in the inextricable connection for RNA remains poorly assessed. We have been able to examine it in tRNA as we show below that the dynamical flexibility is strongly correlated with charge-screening density engendered by hydrated counterions. The additional flexibility of tRNA driven by charge screening alone is examined in terms of $\Delta\langle\varepsilon\rangle$ which is obtained by subtracting the $\langle\varepsilon\rangle$ of dialyzed tRNA from the $\langle\varepsilon\rangle$ of salted tRNA samples (assuming no significant change in hydration-enhanced flexibility between dialyzed and salted samples as long as they are hydrated with similar amount of water molecules, which is rationalized by the similar T_d). Interestingly, $\Delta\varepsilon/T$ turns out to be directly proportional to logarithmic of charge-screening density with unique ζ values extrapolated at zero-point dynamic energy ($\zeta|_{\Delta\langle\varepsilon\rangle=0}$) at each temperature (Fig. 4 and S4, and Table 1). Accordingly, the empirical correlation can be expressed as $\ln(\zeta(T)/\zeta|_{\Delta\langle\varepsilon\rangle=0}(T)) \sim \Delta\langle\varepsilon\rangle/T$, which manifests that the change of dynamic energy factor is reflected by the extent of charge-screening density of hydrated counterions. The presence of nonzero $\zeta|_{\Delta\langle\varepsilon\rangle=0}$ implies that there is a threshold of charge screening enough to trigger the onset of additional conformational exploration on sub-ns timescales. Above the threshold, the relevant dynamic energy probably outcompetes localized structural interactions bridged by hydrated counterions. At 300 K, the electrostatic threshold is about 63% of charge-screening density of hydrated K^+ . Weaker electrostatic interactions at higher temperatures accounts for the decreased $\zeta|_{\Delta\langle\varepsilon\rangle=0}$ with increasing temperature.

Table 1. Charge-screening density of hydrated cations and extrapolated $\zeta|_{\Delta\langle\varepsilon\rangle=0}$ at each temperature.

Cation	ζ^a [$e/\text{\AA}^3$]	T [K]	$\zeta _{\Delta\langle\varepsilon\rangle=0}$ [$e/\text{\AA}^3$] $\times 10^3$
Mg^{2+}	0.055	260	10.71 ± 0.08
Na^+	0.017	280	9.07 ± 0.07
K^+	0.012	300	7.57 ± 0.08

^a $\zeta = 2e/(4\pi/3)R^3$, where R is the radius of hydrated cation.



4 | *Soft Ma*

Fig. 4 Change in dynamic energy factor, $\Delta\langle\varepsilon\rangle$, corresponding to additional conformational motions of wet tRNA driven by charge screening vs. logarithmic charge-screening density of hydrated counterions at 260, 280, and 300 K.

In conclusion, we report that more and denser charge screening (i.e. larger charge-screening density around RNA) engendered by hydrated counterions serves to enhance dynamic flexibility of tRNA, while also inducing structural stabilization. The increased mobility is concomitantly attributed to more mobile fraction of faster conformational motions with larger mobile length scale. A threshold of charge screening that triggers the onset of the additional flexibility is estimated from the correlation between the charge-screening density of the hydrated counterions and the enhanced comprehensive dynamics of tRNA. This implies that larger flexibility of tRNA driven by the greater charge-screening density arises from local conformational relaxation coupled with stabilized charge screening rather than governed by the fluctuation of hydrated counterions.

Notes and references

J.H.R., P.A., and K.K. acknowledge support from Institute for Basic Science (IBS) [IBS-R007-D1]. This work utilized facilities (NCNR High Flux Backscattering Spectrometer) supported in part by the National Science Foundation under Agreement No. DMR-0944772.

- (a) B. F. Rasmussen, A. M. Stock, D. Ringe, and G. A. Petsko, *Nature* 1992, **357**, 423. (b) J. A. Rupley and G. Careri, *Adv. in Protein Chem.*, 1991, **41**, 37. (c) E. Westhof, *Annu. Rev. Biophys. Biophys. Chem.*, 1988, **17**, 125. (d) J. Yoon, J.-C. Lin, C. Hyeon, and D. Thirumalai, *J. Phys. Chem. B*, 2014, **118**, 7910.
- (a) Z. Bu, J. Cook, and D. J. E. Callaway, *J. Mol. Biol.*, 2001, **312**, 865. (b) V. Receveur, P. Calmettes, J. C. Smith, M. Desmadril, G. Coddens, and D. Durand, *Proteins: Struct., Funct., Genet.*, 1997, **28**, 380. (c) E. Mamontov, and H. O'Neill, Q. Zhang, *J. Biol. Phys.*, 2010, **36**, 291.
- (a) P. W. Fenimore, H. Frauenfelder, B. H. McMahon, and F. G. Parak, *Proc. Natl. Acad. Sci. U. S. A.*, 2002, **99**, 16047. (b) A. L. Tournier, J. C. Xu, and J. C. Smith, *Biophys. J.*, 2003, **85**, 1871. (c) K. Wood, A. Frolich, A. Paciaroni, M. Moulin, M. Hartlein, G. Zaccai, D. J. Tobias, and M. Weik, *J. Am. Chem. Soc.*, 2008, **130**, 4586. (d) S. Khodadadi and A. P. Sokolov, *Soft Matter*, 2015, **11**, 4984.
- (a) G. Zaccai, *Philos. Trans. R. Soc. Lond. Ser. B-Biol. Sci.*, 2004, **359**, 1269. (b) S. Khodadadi, J. H. Roh, A. Kisliuk, E. Mamontov, M. Tyagi, S. A. Woodson, R. M. Briber, and A. P. Sokolov, *Biophys. J.*, 2010, **98**, 1321. (c) K. Wood, M. Plazanet, F. Gabel, B. Kessler, D. Oesterhel, D. J. Tobias, G. Zaccai, and M. Weik, *Proc. Natl. Acad. Sci. U. S. A.*, 2007, **104**, 18049. (d) X. Li, M. Zamponi, K. Hong, L. Porcar, C.-Y. Shew, T. Jenkins, E. Liu, G. S. Smith, K. W. Herwig, Y. Liu, and W.-R. Chen, *Soft Matter*, 2011, **7**, 618.
- J. H. Roh, R. M. Briber, A. Damjanovic, D. Thirumalai, S. A. Woodson, and A. P. Sokolov, *Biophys. J.*, 2009, **96**, 2755.
- J. H. Roh, M. Tyagi, R. M. Briber, S. A. Woodson, and A. P. Sokolov, *J. Am. Chem. Soc.*, 2011, **133**, 16406.
- (a) D. E. Draper, D. Grilley, and A. M. Soto, *Annu. Rev. Biophys. Biomol. Struct.*, 2005, **34**, 221. (b) S. Moghaddam, G. Caliskan, S. Chauhan, C. Hyeon, R. M. Briber, D. Thirumalai, and S. A. Woodson, *J. Mol. Biol.*, 2009, **393**, 753.
- (a) M. Kofu, T. Someya, S. Tatsumi, K. Ueno, T. Ueki, M. Watanabe, T. Matsunaga, M. Shibayama, V. Garcia Sakai, and M. Tyagi, *Soft Matter*, 2012, **8**, 7888. (b) S. Khodadadi, S. Pawlus, J. H. Roh, V. G. Sakai, E. Mamontov, and A. P. Sokolov, *J. Chem. Phys.*, 2008, **128**, 195106-1.

This journal is © The Royal Society of Chemistry 20xx

Journal Name

COMMUNICATION

- 9 (a) Y. Mu and G. Stock, *Biophys. J.*, 2006, **90**, 391. (b) Q. Zhang, X. Sun, E. D. Watt, and H. M. Al-Hashimi. *Science*, 2006, **311**, 653.
- 10 (a) M. Tehei, D. Madern, C. Pfister, and G. Zaccai, *Proc. Natl. Acad. Sci. U. S. A.*, 2001, **98**, 14356. (b) M. Mevarech, F. Frolow, L. M. Gloss, *Biophysical Chemistry*, 2000, **86**, 155. (c) M. T. Record, W. Zhang, and C. F. Anderson, *Adv. Protein Chem.*, 1998, **51**, 281.